Application of an Undertow Model to Irregular Waves on Barred Beaches

Douglas L. Kennedy[1], Daniel T. Cox[2] and Nobuhisa Kobayashi[3]

ABSTRACT: An undertow model calibrated for regular waves on plane beaches is applied to predict the irregular wave induced undertow for both plane and barred beaches and for both laboratory and field data sets. The model combines a logarithmic profile in the bottom boundary layer with a conventional parabolic profile in the interior. The height and period of the irregular waves are represented by the local root-mean-square wave height and spectral peak period, and the measured mean volume flux below trough level is used as input to the model. The model is capable of predicting the undertow profiles both inside and outside the surf zone, provided that the empirical coefficient associated with the mean bottom shear stress is adjusted at each measuring line. The model appears to give reasonable predictions of the bottom boundary layer thickness and shear velocity, although these predictions could not be verified due to a lack of data. To develop a predictive undertow model, a simple relationship with an adjustable coefficient is applied to predict the measured volume flux below trough level using the local wave height and water depth. The calibration coefficients involved in the predictive model are not universal among the lab and field conditions possibly due to the effects of wave directionality and longshore currents in the field measurements which are neglected in this paper.

INTRODUCTION

Detailed sediment transport models require accurate prediction of the cross-shore currents or undertow. Most undertow models are based on the time-averaged, cross-shore momentum equation and are verified primarily with laboratory measurements of the undertow induced by regular waves breaking on smooth, plane slopes. Cox and Kobayashi (1996) showed the difficulties inherent in standard undertow models, including the difficulties in obtaining reliable estimates of all the terms in the time-averaged, cross-shore momentum equation. Furthermore, some of these models give no estimate of the undertow in the bottom boundary layer or the mean bottom shear stress. Recently, Cox

[1]Graduate Student, Div. of Coastal and Ocean Engrg., Dept. of Civil Engrg., Texas A&M Univ., College Station, TX 77843-3136.
[2]Asst. Prof., Div. of Coastal and Ocean Engrg., Dept. of Civil Engrg., Texas A&M Univ., College Station, TX 77843-3136; Email: dtc@arlo.tamu.edu
[3]Prof. and Assoc. Dir., Center for Applied Coastal Res., Univ. of Delaware, Newark, DE 19716.

and Kobayashi (1997) developed a new undertow model without relying on the time-averaged momentum equation. They calibrated and verified the model using laboratory data of regular waves breaking on rough and smooth plane slopes. The model was found to give accurate predictions of the undertow profiles inside and outside the surf zone, provided that the empirical coefficient associated with the mean bottom shear stress was calibrated at each measuring line.

This paper extends their work by applying the model to predict undertow induced by irregular waves breaking over plane and barred beaches using both laboratory and field data. Additionally, this paper shows how the mean volume flux below trough level, which is an input to the model, may be predicted from the local root-mean-square wave height and water depth. This paper is organized as follows. The model is briefly summarized, and the data sets used for comparison are discussed. Comparisons are then presented for undertow profiles and the mean volume flux below trough level along with a discussion of the calibration coefficients and model sensitivity. The performance of the model is summarized at the end with a discussion of the implications of the coefficients.

UNDERTOW MODEL

The undertow model was presented in detail in Cox and Kobayashi (1997) and is summarized herein to facilitate the comprehension of the subsequent comparisons. The model combines a conventional parabolic profile in the interior with a logarithmic profile in the bottom boundary layer. The undertow $\overline{u}$ from the bottom to trough level is expressed as

$$\overline{u} = \frac{\overline{u_*}}{\kappa} \ln\left(\frac{z_b}{z_0}\right) \quad \text{for} \quad z_0 \leq z_b \leq \delta \tag{1}$$

and

$$\overline{u} = \overline{u}_b + \alpha z_b{}^2 \quad \text{for} \quad \delta < z_b \leq d_t \tag{2}$$

where $\overline{u_*}$ = mean shear velocity; κ = von Kármán constant, taken as $\kappa = 0.4$ in this paper; z_0 = bottom roughness height; z_b = vertical coordinate above the bottom, positive upward with $z_b = 0$ on the bottom; $\overline{u}_b$ = hypothetical undertow velocity in the absence of the boundary layer; δ = boundary layer thickness; d_t = water depth below trough level; and α = dimensional coefficient to be expressed in terms of the physical variables.

For smooth slopes typical of laboratory experiments, the roughness height is specified as $z_0 = \nu/(9\,\overline{u_*})$ based on unidirectional flow where ν is the kinematic viscosity. For rough slopes in the absence of bed forms, $z_0 = 2\,d_{50}/30$ based on the analysis of regular waves breaking on a plane, rough slope where d_{50} is the median grain diameter. Estimates of z_0 for the field data are more difficult due to the presence of ripples and megaripples and are explained later.

An expression for the mean shear velocity $\overline{u_*}$ in (1) is developed using the quadratic friction equation for the temporal variation of the bottom shear stress τ_b given by

$$\tau_b = \frac{1}{2}\rho\,f_b\,|u_b|\,u_b \tag{3}$$

where ρ = fluid density; f_b = constant bottom friction factor; and u_b = instantaneous horizontal velocity at the bottom in the absence of the boundary layer. For normally

incident regular waves, u_b may be expressed as a sum of the sinusoidal wave component and the mean component $\overline{u}_b$ and is given as

$$u_b = U_b \cos(kx - \omega t) + \overline{u}_b \tag{4}$$

where k = local wave number; x = horizontal coordinate, positive onshore; ω = angular wave frequency; and t = time. The amplitude U_b of the wave component in (4) is based on linear wave theory and is given as (e.g., Jonsson, 1966)

$$U_b = \frac{H\,\omega}{2\,\sinh(k\overline{h})} \tag{5}$$

where H = local wave height, and $\overline{h}$ = local water depth including the setup. Substituting (4) into (3) and taking the time-average with the assumption of a small current $(\overline{u}_b/U_b)^2 \ll 1$, the mean bottom shear stress $\overline{\tau}_b$ may be given as

$$\overline{\tau}_b \simeq \frac{2}{\pi}\,\rho\,f_b\,U_b\,\overline{u}_b \tag{6}$$

Defining the mean shear velocity by $|\overline{u_*}|\,\overline{u_*} = \overline{\tau}_b/\rho$ together with (6) yields

$$\overline{u_*} = (C_*\,f_b\,U_b\,|\overline{u}_b|)^{1/2}\,\frac{\overline{u}_b}{|\overline{u}_b|} \tag{7}$$

in which C_* = empirical coefficient calibrated later. It is noted that $C_* \simeq 2/\pi$ if (3) and linear wave theory are accurate enough to estimate the relatively small value of $\overline{u_*}$, and it is further noted that the time-averaged bottom boundary layer is much less understood than the oscillatory bottom boundary layer.

The bottom friction factor f_b in (7) may be estimated for rough slopes as (Jonsson, 1966)

$$\frac{1}{4\sqrt{f_b}} + \log\frac{1}{4\sqrt{f_b}} = \log\left(\frac{A_b}{k_s}\right) - 0.08 \tag{8}$$

and for smooth slopes as (Kamphuis, 1975)

$$\frac{1}{8.1\sqrt{f_b}} + \log\frac{1}{\sqrt{f_b}} = \log\sqrt{Re} - 0.135 \tag{9}$$

where A_b = excursion amplitude given by $A_b = U_b/\omega$; k_s = equivalent roughness taken as $k_s = 30\,z_0$; and Re = Reynolds number defined as $Re = U_b\,A_b/\nu$.

Assuming that the thickness of the undertow boundary layer is approximately equal to the thickness of the wave boundary layer, the boundary layer thickness δ in (1) and (2) may be approximated by (Grant and Madsen, 1979)

$$\delta = C_\delta\,\frac{\kappa\,(u_*)_{max}}{\omega} \tag{10}$$

where $(u_*)_{max}$ = maximum shear velocity over the wave period; and C_δ = empirical constant in the range $1 \leq C_\delta \leq 2$ and is taken as $C_\delta = 1.5$ in this paper because the predicted results have been found to be insensitive to C_δ in this range. The maximum shear velocity $(u_*)_{max}$ in (10) is estimated by taking the maximum of (3) using (4)

and employing the small current assumption used to derive (7). Substitution of this expression into (10) yields

$$\delta = C_\delta \left(\frac{\kappa}{\omega}\right) \left[\frac{1}{2} f_b U_b \left(U_b + 2|\overline{u}_b|\right)\right]^{1/2} \tag{11}$$

The coefficient α in (2) can be obtained by matching (1) and (2) at $z_b = \delta$ which yields

$$\alpha = \frac{1}{\delta^2} \left[\frac{\overline{u_*}}{\kappa} \ln\left(\frac{\delta}{z_0}\right) - \overline{u}_b\right] \tag{12}$$

To close the problem, the mean volume flux below trough level, Q_t, is specified and is estimated from the measured undertow profile in this paper. The prediction of Q_t will be addressed separately at the end of this section. The volume flux is defined as

$$Q_t = \int_{z_0}^{d_t} \overline{u}\, dz_b \tag{13}$$

where Q_t is negative for the undertow $\overline{u}$. Substituting (1) and (2) into (13) and solving for $\overline{u}_b$ gives

$$\overline{u}_b = \frac{1}{d_t} \left[Q_t + \frac{\overline{u_*}}{\kappa}\delta - \frac{\alpha}{3}\left(d_t^3 + 2\delta^3\right)\right] \tag{14}$$

The solution of (1), (2), (7), (11), and (12) with (14) is termed Method 1.

In light of the uncertainty in estimating the relatively small $\overline{u_*}$ using the time-averaging of the quadratic equation (3), a second method is proposed to estimate $\overline{u_*}$ directly from $\overline{u}_b$ without regard to the oscillatory wave velocity. Instead of (7), $\overline{u_*}$ is assumed to be expressed as

$$|\overline{u_*}|\, \overline{u_*} = \frac{1}{2} \overline{f}\, |\overline{u}_b|\, \overline{u}_b \tag{15}$$

in which $\overline{f}$ = empirical friction factor for the undertow assumed to be given by $\overline{f} = C_f f_b$ where C_f is an empirical coefficient. It is noted that $C_f = 1$ if the friction factors $\overline{f}$ and f_b for the undertow and wave induced velocity are the same. From (15), the mean shear velocity is given by

$$\overline{u_*} = \sqrt{0.5\, C_f\, f_b}\;\; \overline{u}_b \tag{16}$$

Since (16) does not require the small current assumption used in (7), $(\tau_b)_{max}$ is derived from (3) without this assumption and is given as

$$(\tau_b)_{max} = \rho\, [(u_*)_{max}]^2 = \frac{1}{2} \rho\, f_b \left(U_b + |\overline{u}_b|\right)^2 \tag{17}$$

Substitution of (17) into (10) for the boundary layer thickness gives

$$\delta = C_\delta \left(\frac{\kappa}{\omega}\right) \sqrt{\frac{f_b}{2}} \left(U_b + |\overline{u}_b|\right) \tag{18}$$

In short, $\overline{u_*}$ and δ estimated by (7) and (11) in Method 1 are replaced by (16) and (18) in Method 2. Since C_δ is fixed, each method has only one primary calibration coefficient: C_* for Method 1 and C_f for Method 2. These methods may not be satisfactory

physically, but they are necessary to estimate the mean shear velocity $\overline{u_*}$ whose data appears to be limited, especially inside the surf zone.

The above undertow model developed originally for normally-incident regular waves may also be applied to normally-incident irregular waves by approximating the irregular waves by the equivalent regular waves based on the local root-mean-square wave height, H_{rms}, and the spectral peak period, T_p. The use of H_{rms} may be appropriate because the mean volume flux Q_t given by (13) is approximately proportional to the square of the local wave height as explained below. The choice of the spectral peak period is somewhat arbitrary, but this period is typically reported for irregular wave data. For field data, the cross-shore fluid motion under directional random waves may be approximated by that under normally-incident random waves if $\theta_c{}^2 \ll 1$ where θ_c is the characteristic incident angle in radians. The assumption of $\theta_c{}^2 \ll 1$ is usually satisfied in the surf zone because of wave refraction. However, longshore currents may not be negligible even if $\theta_c{}^2 \ll 1$ and may affect the mean cross-shore bottom shear stress in view of the cross-shore sediment transport analysis using field data by Thornton *et al.* (1996). Consequently, the subsequent comparisons with field data will need to be interpreted bearing this limitation in mind.

The use of the measured volume flux Q_t below trough level implies that this undertow model predicts the undertow profile but can not be used to predict the magnitude of the undertow. To address this shortcoming, an attempt is made to estimate Q_t from the local root-mean-square wave height, H_{rms}, and local water depth, $\bar{h} = (d + \bar{\eta})$, where $d = $ still water depth and $\bar{\eta} = $ setup. The volume flux below trough level is approximated as

$$Q_t \simeq \overline{U} d_t \tag{19}$$

where $\overline{U} = $ depth-averaged velocity estimated by

$$\overline{U} \simeq -\frac{C_u \sqrt{g\bar{h}}}{8} \left(\frac{H_{rms}}{\bar{h}} \right)^2 \tag{20}$$

where $g = $ gravitational acceleration, and $C_u = $ empirical coefficient introduced herein to account for the roller effect. The roller effect is expected to increase the magnitude of $\overline{U}$ inside the surf zone. Equation (20) with $C_u = 1$ can be derived from the time-averaged continuity equation together with the assumption of linear progressive long waves where H_{rms} is defined as $H_{rms} = \sqrt{8}\,\sigma$ with $\sigma = $ standard deviation of the free surface elevation. It is further noted that cross-shore variation in wave height and setup could be predicted using the time-averaged equations for momentum and energy.

SUMMARY OF DATA SETS

Table 1 summarizes the data sets used for comparison with the undertow model, indicating the literature cited, the data set name from each paper, and the abbreviation used in this paper. The data are comprised of both laboratory and field conditions, and the undertow is induced by irregular waves for all cases. The fifth through eighth columns indicate the quantities used to compute the surf similarity parameter given by

$$\xi = \frac{\tan \alpha}{\sqrt{H_{rms}/L_p}} \tag{21}$$

where α = local beach slope, and L_p = local wavelength computed using linear wave theory with the peak period, T_p. For the first five cases, ξ is estimated at the most seaward measuring line as shown in the subsequent figures. For the last two cases, ξ is estimated at the fifth measuring line since the first four seaward measuring lines had a very gentle slope. The range of the surf similarity parameter for the seven cases listed in Table 1 is $0.22 \le \xi \le 0.44$, indicating spilling and plunging waves with little reflection of wind waves. It is noted that the definition of H_{rms} for these data sets was not clearly stated in all cases. As a result, the values of H_{rms} based on the standard deviation σ, the spectral method, and the zero-crossing method are assumed to be the same.

Table 1: Summary of irregular wave induced undertow data for comparison with the undertow model.

Literature Cited	Abbr.	Lab or Field	Bathy.	$\tan \alpha$	H_{rms} (cm)	T_p (s)	$\bar{h}$ (cm)	ξ
Sultan (1995)	S95	Lab	P, S	1:35	7.1	3.0	28.9	0.24
Okayasu and Katayama (1992)	OK92	Lab	B, S	1:20	7.6	1.14	20.0	0.22
Smith *et al.* (1992)	SSP92-A	Field	B, R	1:22	59	9.7	230	0.38
Smith *et al.* (1992)	SSP92-B	Field	B, R	1:23	61	5.6	190	0.26
Smith *et al.* (1992)	SSP92-C	Field	B, R	1:28	65	7.0	221	0.25
Haines and Sallenger (1994)	HS94-A	Field	B, R	1:22	99	13.3	145	0.32
Haines and Sallenger (1994)	HS94-B	Field	B, R	1:18	101	14.4	200	0.44

Note: P=Plane, B=Barred; S=Smooth, R=Rough

Cox and Kobayashi (1997) compared the undertow model to the measured undertow induced by regular waves on plane slopes in the laboratory. The first extension of this paper is to compare the model to laboratory undertow data for irregular waves on a plane slope (Sultan, 1995), and then for irregular waves on a triangular barred profile (Okayasu and Katayama, 1992). These laboratory tests were for normally incident irregular waves with no longshore current. The next extension is to compare the model to the field data of Smith *et al.* (1992) and Haines and Sallenger (1994). The field measurements were collected on a barred beach at the USACE Field Research Facility in Duck, North Carolina, under a fairly uniform bathymetry in the longshore direction (e.g., Smith *et al.*, 1992). Although the longshore current was not reported in Smith *et al.* (1992), the peak incident wave angle measured counter-clockwise from shore normal was given as $\theta = -15$, -43, and $+24$ degrees at 8 m depth for SSP92-A, SSP92-B, and SSP92-C. Nevertheless, Smith *et al.* (1992) compared their undertow model for essentially normally-incident waves with these data sets apart from an empirical correction of $\cos \theta$ in (20) with $C_u = 2.4$.

Haines and Sallenger (1994) reported the magnitude and direction of the longshore current for HS94-A and HS94-B. For HS94-A, the magnitude of the longshore current was generally less than the cross-shore current, but the longshore current was not unidirectional. For HS94-B, the magnitude of the longshore current was approximately on

the same order as the cross-shore current and was unidirectional. Haines and Sallenger (1994) compared their undertow model for normally-incident waves with their data sets, excluding one data set with vigorous longshore currents. It is noted that none of the data sets mentioned above included detailed measurements of the undertow and shear stress in the bottom boundary layer.

UNDERTOW PROFILES

The undertow model is compared with the seven data sets listed in Table 1 using the measured volume flux below trough level to close the system of equations as described above. The volume flux is estimated by integrating a cubic spline fitted through the measured points. For both Method 1 and Method 2, the calibration coefficients are adjusted at each measuring line to give a best fit "by eye" to the data.

Table 2 lists the input parameters to the model at each measuring line for the data of Sultan (1995) where η_{tr} = negative trough elevation relative to the still water level which is used to calculate $d_t = (d + \eta_{tr})$. Since the trough level η_{tr} was not given in Sultan (1995), η_{tr} was taken as the elevation where the undertow changed sign from negative to positive below the still water level. This elevation corresponds roughly to $0.3 H_{rms}$; and it is noted that the ratio of $|\eta_{tr}/H| \simeq 0.3$ was found for the regular wave data of Cox and Kobayashi (1996), Nadaoka and Kondoh (1982), and Hansen and Svendsen (1984). Column 8 indicates the amplitude of the orbital velocity U_b based on linear wave theory; and for the cases presented here, the small current assumption $(\overline{u}_b/U_b)^2 << 1$ used in (6) is reasonable. Column 9 gives the Reynolds number used to estimate the friction factor f_b in Column 10 using (9) for the smooth slope, which are in the range $0.8 \times 10^4 \leq Re \leq 4.1 \times 10^4$ and $0.011 \leq f_b \leq 0.017$.

Table 2: Model input and calibration coefficients for S95.

Line	d	H_{rms}	$\overline{\eta}$	η_{tr}	Q_t	$k\overline{h}$	U_b	Re	f_b	C_*	C_f	C_u
No.	(cm)	(cm)	(cm)	(cm)	(cm^2/s)		(cm/s)	$\times 10^{-4}$	$\times 10^{-2}$			
S1	29.0	7.1	-0.11	-3.2	-49	0.367	19.8	1.6	1.4	0.060	1.2	1.5
S2	23.3	8.1	-0.15	-2.6	-44	0.327	25.5	2.7	1.2	0.060	1.3	0.9
S3	20.8	8.6	-0.17	-1.8	-45	0.308	28.8	3.4	1.1	0.060	1.3	0.8
S4	17.7	8.6	-0.16	-1.9	-39	0.283	31.4	4.1	1.1	0.060	1.3	0.6
S5	16.1	8.1	-0.14	-2.1	-46	0.271	31.0	4.0	1.1	0.060	1.2	0.8
S6	14.4	7.2	-0.13	-2.1	-36	0.256	29.2	3.5	1.1	0.070	1.1	0.8
S7	13.1	6.5	-0.09	-1.5	-44	0.243	27.8	3.2	1.2	0.080	1.0	1.1
S8	12.1	6.1	-0.01	-1.2	-41	0.229	27.6	3.2	1.2	0.090	1.0	1.1
S9	9.7	5.3	0.09	-1.3	-45	0.209	26.3	2.9	1.2	0.110	1.8	1.5
S10	7.7	4.2	0.23	-1.0	-29	0.186	23.5	2.3	1.3	0.120	1.8	1.5
S11	5.6	3.3	0.40	-1.1	-25	0.164	21.0	1.8	1.4	0.130	1.7	1.9
S12	3.1	1.7	0.66	0.0	-16	0.128	13.8	0.8	1.7	0.170	1.6	3.4

Columns 11 and 12 give the calibration coefficients C_* for Method 1 and C_f for Method 2. C_* increases shoreward as was found in Cox and Kobayashi (1997) for the regular wave comparisons, but the variation in C_* from outside the surf zone to inside the surf zone is less pronounced for the irregular wave case. The magnitude of

C_* is 0.1 which is much less than $(2/\pi) = 0.64$, indicating that (6) overpredicts the mean bottom shear stress as was found by Cox and Kobayashi (1997). C_f generally decreases shoreward as was also noted in Cox and Kobayashi (1997); however, C_f increases unexpectedly in the inner surf zone. Overall, the magnitude of C_f is on the order of 1.0, indicating that $\overline{f} \simeq f_b$. Column 13 gives the values of C_u in (20) which are discussed later in relation to the prediction of the volume flux below trough level.

Figure 1 compares the model predictions with the measurements of Sultan (1995). Trough level is indicated in the figure by the vertical extent of the model predictions. The horizontal extent from S1 to S12 is approximately 9 m. The figure indicates that the model predicts the measured undertow profile below trough level both outside and inside the surf zone for both methods with the coefficients adjusted at each measuring line. The boundary layer thickness is estimated by the model to be in the range $0.5 \le \delta \le 0.7$ cm, and the mean shear velocity is estimated to be in the range $-0.5 \le \overline{u_*} \le -0.2$ cm/s over the 12 measuring lines for Methods 1 and 2. These ranges indicate the difficulty in measuring the undertow and mean shear velocity in the bottom boundary layer in the laboratory. Figure 2 shows the model sensitivity to a 20% variation in C_*. In this figure, the adopted C_* at each measuring line is shown by a solid line whereas $0.8\,C_*$ and $1.2\,C_*$ are shown by dashed and dash-dot lines, respectively. A similar variation in the undertow profiles is achieved for only a 5% variation in C_f, and the figure is not shown for brevity.
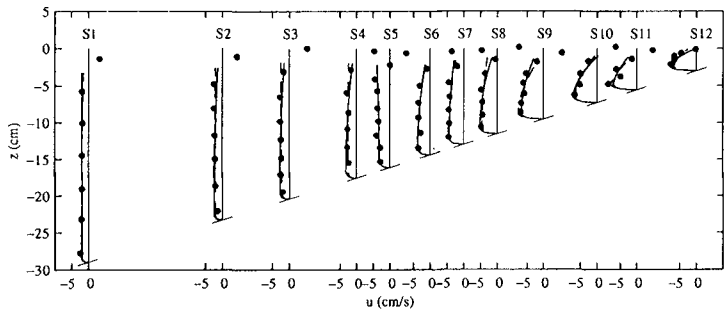
Figure 1: Model predictions for S95: Measured $\overline{u}$ (•); Predicted, Method 1 (——); and Predicted, Method 2 (– –).

For the data of Okayasu and Katayama (1992), the local H_{rms} is estimated by $H_s = \sqrt{2}\,H_{rms}$ where the significant wave height H_s is taken from the significant crest and trough elevations, $(\eta_{cr})_s$ and $(\eta_{tr})_s$, reported in their paper. Figure 3 compares the model and data for both methods. In this figure, the horizontal extent from O1 to O6 is approximately 5 m, and the triangular bar consists of three linear segments. Figure 3 indicates that the model predicts the undertow profile over a barred bathymetry as well, apart from the scatter of data points at O6, provided that the coefficients are adjusted at each measuring line. For this case, the boundary thickness is estimated to be in the range $0.2 \le \delta \le 0.4$ cm, and the mean shear velocity is estimated to be in the range $-0.4 \le \overline{u_*} \le -0.05$ cm/s.
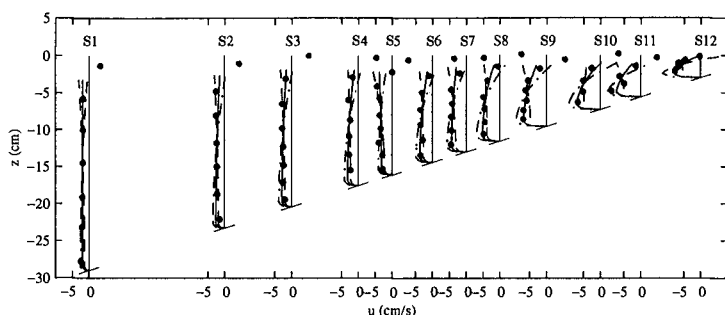
Figure 2: Model sensitivity for S95: Measured $\overline{u}$ (●); Predicted, Method 1 with adopted C_* (——); Predicted, Method 1 with $0.8\,C_*$ (– –); and Predicted, Method 1 with $1.2\,C_*$ (– · –).

For comparisons with the data of Smith *et al.* (1992), the local H_{rms} for each of the six measuring lines is obtained by a linear interpolation of the measured values in their paper. Although the local setup $\overline{\eta}$ was not measured, $\overline{\eta}$ was estimated in Smith *et al.* (1992); and the ratio of this estimated setup to the minimum local water depth was approximately 0.03 for the three cases. Therefore, $\overline{\eta}$ is neglected here, and the approximation $\overline{h} \simeq d$ is assumed for input in the undertow model. The trough level was also not reported, and the crude approximation of $\eta_{tr} \simeq 0.3\,H_{rms}$ is used here. The relative roughness in (8) is found to be in the range $29 \leq A_b/k_s \leq 73$ for the three cases where the roughness height is assumed as $z_0 = 0.05$ cm and $k_s = 30\,z_0 = 1.5$ cm for lack of data on bed forms. The Reynolds number is found to be in the range $2.1 \times 10^5 \leq Re \leq 7.8 \times 10^5$ for the field data. This range of relative roughness and Reynolds number indicates that the flow in the bottom boundary layer is rough turbulent even without the turbulence generated by wave breaking (Jonsson, 1966). The friction factor was found to be in the range $0.025 \leq f_b \leq 0.038$ which is larger than $f_b = 0.01$ specified in Smith *et al.* (1992) for their model comparisons. However, the use of a much smaller value for z_0 would reduce f_b. For example, $z_0 = 0.007$ cm would yield the range $0.012 \leq f_b \leq 0.016$.

For a given case, C_* varies at each measuring line; but for a given measuring line, C_* is fairly constant for the three cases. Compared to the laboratory cases with regular waves, there is less cross-shore variation in C_* for a given case, although it is noted that the field measurements do not include the inner surf zone near the still water shoreline. The variation in C_f at a given measuring line for the three cases is also small. The values of C_* and C_f for these field data are smaller than the corresponding values of C_* and C_f listed in Table 2 for the laboratory data of Sultan (1995). (Table 4 compares the average calibration coefficients for all cases listed in Table 1). The mean shear velocity $\overline{u_*}$ given by (7) and (16) depends on C_*f_b and $C_f f_b$, respectively, instead of f_b itself. The calibrated values of C_* and C_f depends on the adopted value of z_0 which affects f_b somewhat, but the values of C_*f_b and $C_f f_b$ remain approximately the same. In other words, the change of z_0 by a factor of 10 will change f_b, C_*, and C_f by roughly a factor of 2.
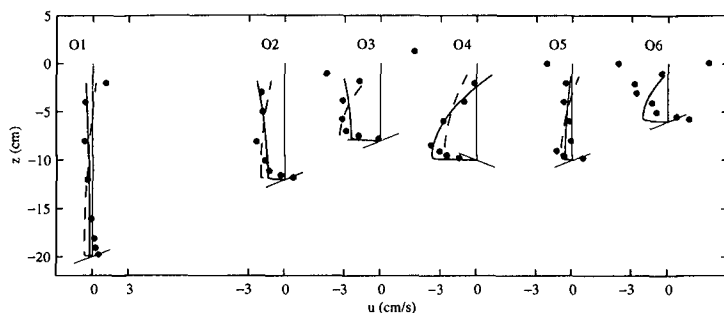
Figure 3: Model predictions for OK92: Measured $\overline{u}$ (•); Predicted, Method 1 (——); and Predicted, Method 2 (— —).
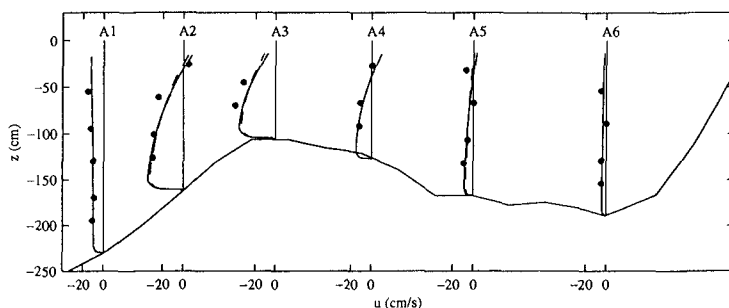
Figure 4: Model predictions for SSP92-A: Measured $\overline{u}$ (•); Predicted, Method 1 with adopted C_* (——); and Predicted, Method 1 with C_{*ave} (— —).

Figure 4 compares the undertow model for Method 1 with the data of SSP92-A using C_* calibrated at each measuring line and the average C_* values for the three cases. The horizontal extent from A1 to A6 is approximately 100 m. Figure 4 indicates that the model predicts the undertow profile over a barred beach for field conditions, provided that the coefficients are adjusted at each measuring line. The values of C_* are larger at A2 and A3 located immediately seaward and on the bar crest, respectively, whereas the values of C_f do not change much across the barred beach. The agreement for Method 2 and for the two other cases SSP92-B and SSP92-C is similar, and the figures are not shown for brevity. For these field data, the boundary layer thickness is estimated to be in the range $4 \le \delta \le 11$ cm, and the mean shear velocity is estimated to be in the range $-2.1 \le \overline{u_*} \le -0.2$ cm/s. These values are much larger than the laboratory values estimated for S95 and OK92.

Similar to Smith et al. (1992), $\overline{\eta}$ and η_{tr} were not given in the paper of Haines and Sallenger (1994), and the assumptions of $\overline{h} \simeq d$ and $\eta_{tr} \simeq 0.3 H_{rms}$ are made here as well. The roughness height is assumed as $z_0 = 0.05$ cm, and the relative roughness is found to be in the range $88 \le A_b/k_s \le 180$. The Reynolds number is found to be in the
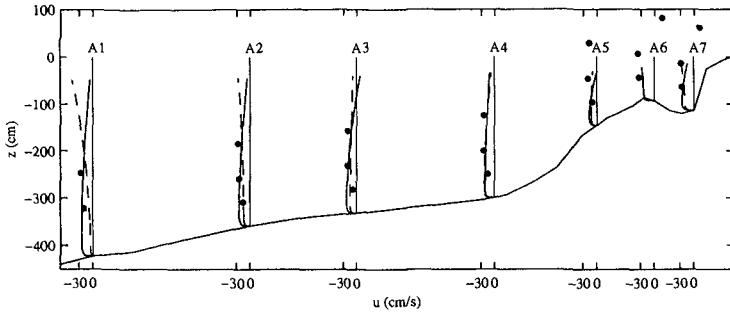
Figure 5: Model predictions for HS94-A: Measured $\bar{u}$ (•); Predicted, Method 1 (——); and Predicted, Method 2 (— —).
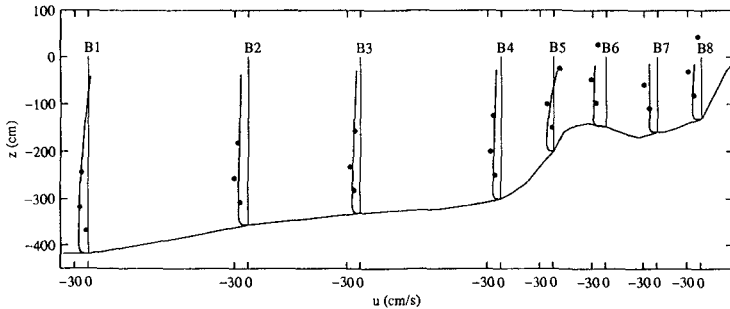
Figure 6: Model predictions for HS94-B: Measured $\bar{u}$ (•); Predicted, Method 1 (——); and Predicted, Method 2 (— —).

range $8 \times 10^5 \leq Re \leq 34 \times 10^5$, indicating rough turbulent flow in the bottom boundary layer (Jonsson, 1966). The cross-shore variations in C_* and C_f are small compared to the laboratory cases.

Figures 5 and 6 show the model agreement for HS94-A and HS94-B. The horizontal extent from A1 to A7 and from B1 to B8 is approximately 300 m. Substantial offshore migration of the bar occurred from October 11 (HS94-A) to October 12 (HS94-B) as explained in Haines and Sallenger (1994). The agreement is good for both methods and for both cases with the calibration coefficients adjusted at each measuring line. For these two cases, the boundary thickness is estimated to be in the range $11 \leq \delta \leq 17$ cm, and the mean shear velocity is estimated to be in the range $-1.5 \leq \overline{u_*} \leq -0.8$ cm/s. These ranges are similar to the field data of SSP92.

VOLUME FLUX BELOW TROUGH LEVEL

As an alternative to specifying the volume flux below trough level using the measurement, the local depth-averaged velocity $\overline{U}$ is estimated using (20) with the measured values of H_{rms} and $\bar{h}$ at the same location. The predictability of the depth-averaged

velocity is discussed in terms of the calibration coefficient C_u which is obtained from (20) using the measured depth-averaged velocity given by $\overline{U} = (Q_t/d_{tr})$ together with the measured values of H_{rms} and $\overline{h}$. If the calibrated values of C_u are fairly constant, (20) may be applied to predict $\overline{U}$. Furthermore, the calibrated values of C_u can be used to assess the roller effect on C_u since $C_u = 1$ assuming no roller effect.

The calibrated values of C_u listed in Table 2 for S95 indicate that C_u is on the order of 1 over most of the shoaling and surf zone. For S9 to S12 in the inner surf zone, C_u is larger than 1, possibly due to the roller effect. The calibrated values of C_u for OK92 are generally less than 1. It is possible that the value of H_{rms} estimated from the significant crest and trough elevations reported by Okayasu and Katayama (1992) may not be very accurate. Noting that $\overline{U}$ is proportional to H_{rms}^2, this estimation error may have resulted in the unexpectedly small values of C_u for OK92. On the other hand, the calibrated values of C_u in for the field data of SSP92 are mostly on the order of unity and tend to be larger over the bar crest region and smaller in the bar trough region in view of the measuring line locations shown in Figure 4. The calibrated values of C_u for HS94 are also on the order of unity for both cases, but C_u tends to be smaller for HS94-A which had a smaller longshore current than HS94-B.

Table 3 summarizes the calibrated values of C_u. The value $\overline{C_u}$ indicated in the table is estimated for each data set by averaging the C_u values over the measuring lines that have qualitatively similar locations in the cross-shore direction, namely outside the surf zone, the breaker zone, the bar-trough zone, and the inner surf zone. In general, Table 3 shows that $\overline{C_u}$ is closer to unity for the laboratory data sets of S95 and OK92 than for the field data sets of SSP92 and HS94. There appears to be no systematic variation of $\overline{C_u}$ in the cross-shore direction as may be expected from the effect of rollers associated with regular breaking waves. For the irregular wave data in the laboratory, the roller effect is not very pronounced; and $C_u = 1$ is a reasonable approximation. For the field data, $\overline{C_u}$ tends to be larger than unity, and the magnitude of the undertow velocities may have been modified by the wave directionality and alongshore variation of wave and current fields.

Table 3: Summary of calibrated values of C_u.

Data Set	Outside surf zone		Breaker zone		Bar/trough zone		Inner surf zone	
	Line	$\overline{C_u}$	Line	$\overline{C_u}$	Line	$\overline{C_u}$	Line	$\overline{C_u}$
S95	S1,S2	1.2	S3-S5	0.7	N/A[1]		S9-S12	2.1
OK92	O1	0.3	O2,O3	0.6	O4-O6	0.7	N/A[2]	
SSP92-A	A1	2.7	A2,A3	3.2	A4-A6	1.3	N/A[2]	
SSP92-B	B1	1.9	B2,B3	2.6	B4-B6	1.1	N/A[2]	
SSP92-C	C1	1.6	C2,C3	3.5	C4-C6	1.6	N/A[2]	
HS94-A	A1-A4	1.5	A5,A6	0.8	A7	2.8	N/A[2]	
HS94-B	B1-B4	2.1	B5	0.5	B6-B8	3.7	N/A[2]	

[1] Trough region not applicable to data of S95

[2] No inner surf zone measurements for these data sets

CONCLUSIONS

Existing undertow models based on a local balance of the horizontal momentum equa-

tion can predict the order of magnitude of the undertow if empirical parameters are calibrated for each data set. Moreover, the literature is divided among regular or irregular waves and laboratory or field conditions with each model typically calibrated for one of these condition only. Rarely is it shown whether the empirical input is universal. For example, Okayasu and Katayama (1992) used empirically adjusted representative wave heights to get reasonable agreement with a model which was calibrated in an earlier paper under similar laboratory conditions. Haines and Sallenger (1994) employed a vertically uniform eddy viscosity which varied at each measuring line, and they attempted to parameterize this variation using their field data only.

Table 4 summarizes the types of data sets considered in this paper and in Cox and Kobayashi (1997), listing the average calibration coefficients with the standard deviation given in parenthesis. These averages are crude in that they do not distinguish between breaking and nonbreaking waves, but they serve to indicate the variability of the coefficients for the different data sets. Table 4 indicates that C_* and C_f are similar for both regular and irregular waves in the laboratories. For all of the data sets, Method 2 using C_f appears to be the most consistent in terms of the small standard deviation relative to the mean value. It was noted earlier in this paper and in Cox and Kobayashi (1997), however, that the predicted undertow is more sensitive to small changes in the calibration coefficient C_f for Method 2 than C_* for Method 1.

Table 4: Summary of calibration coefficients.

Literature Cited	Lab/ Field	Wave Cond.	Bathy.	C_*		C_f		C_u	
Sultan (1995)	Lab	Irreg	P, S	0.09	(.04)	1.0	(.2)	1.3	(.8)
Okayasu and Katayama (1992)	Lab	Irreg	B, S	0.06	(.02)	1.4	(.4)	0.6	(.3)
Smith et al. (1992)	Field	Irreg	B, R	0.03	(.02)	0.22	(.01)	2.0	(1.1)
Haines and Sallenger (1994)	Field	Irreg	B, R	0.03	(.01)	0.61	(.02)	2.0	(1.1)
Cox et al. (1995)	Lab	Reg	P, R	0.05	(.03)	0.47	(.04)	—	—
Hansen and Svendsen (1984)	Lab	Reg	P, S	0.10	(.04)	1.0	(.3)	—	—
Nadaoka and Kondoh (1982)	Lab	Reg	P, S	0.10	(.05)	0.9	(.2)	—	—

Note: P=Plane, B=Barred; S=Smooth, R=Rough

The consistency of the average values of C_u between the two field data sets suggests that (20) with $C_u \simeq 2$ might yield reasonable approximations of the depth-averaged undertow velocity $\overline{U}$, but the standard deviation is 1.1 and fairly large. The values of C_* and C_f for the field data tend to be smaller than those for the laboratory data, but these values of C_* and C_f are affected somewhat by the adopted value of z_0 as well as by the presence of longshore currents. Furthermore, errors associated with use of the model where the volume flux and calibration coefficients are not known are approximately 100% or roughly a factor of 2.

Finally, the values of C_* for all the data sets in Table 4 are definitely less than $C_* = (2/\pi) = 0.64$ based on (6). Consequently, (6) overpredicts the mean bottom

shear stress. The alternative equation (16) with $\bar{f} = C_f f_b$ has been proposed by Cox and Kobayashi (1997) to mitigate the shortcomings of (6), but (16) is physically unsatisfactory because it neglects wave effects. Therefore, it may be concluded that the mean cross-shore bottom shear stress is poorly understood. The state of the art for the alongshore bottom shear stress in the surf zone is similar (e.g. Garcez Faria *et al.*, 1998).

ACKNOWLEDGMENTS

REFERENCES

Cox, D.T. and Kobayashi, N., 1996. Undertow profiles in the bottom boundary layer under breaking waves. *Proc. 25th Int. Conf. on Coastal Engrg.*, ASCE, 3, 3194–3206.

Cox, D.T. and Kobayashi, N., 1997. A kinematic undertow model with a logarithmic boundary layer. *J. Waterway, Port, Coastal, and Ocean Engrg.*, 123 (6), 354–360.

Garcez Faria, A.F., Thornton, E.B., Stanton, T.P., Soares, C.V. and Lippmann, T.C.. 1998 Vertical profiles of longshore currents and related bed shear stress and bottom roughness. *J. Geophys. Res.*, 103 (C2), 3217–3232.

Grant, W.D. and Madsen, O.S., 1979. Combined wave and current interaction with a rough bottom. *J. Geophys. Res.*, 84 (C4), 1797–1808.

Haines, J.W. and Sallenger, A.H., 1994. Vertical structure of mean cross-shore currents across a barred surf zone. *J. Geophys. Res.*, 99 (C7), 14223–14242.

Hansen, J.B. and Svendsen, I.A., 1984. A theoretical and experimental study of undertow. *Proc. 19th Int. Conf. on Coastal Engrg.*, ASCE, 2246–2262.

Jonsson, I.G., 1966. Wave boundary layers and friction factors. *Proc. 10th Int. Conf. on Coastal Engrg.*, ASCE, 127–148.

Kamphuis, J.W., 1975. Friction factor under oscillatory waves. *J. Waterway, Harbors and Coastal Engrg.*, 101 (2), 135–144.

Nadaoka, K. and Kondoh, T., 1982. Laboratory measurements of velocity field structure in the surf zone by LDV. *Coastal Engrg. in Japan*, 25, 125–145.

Okayasu, A. and Katayama, H., 1992. Distribution of undertow and long-wave component velocity due to random waves. *Proc. 23rd Int. Conf. on Coastal Engrg.*, ASCE, 883–893.

Smith, J.M., Svendsen, I.A., and Putrevu, U., 1992. Vertical structure of the nearshore current at DELILAH: Measured and modeled. *Proc. 23rd Int. Conf. on Coastal Engrg.*, ASCE, 2825–2838.

Sultan, N., 1995. Irregular wave kinematics in the surf zone. Ph.D. Dissertation, Texas A&M University, College Station, Texas.

Thornton, E.B., Humiston, R.T., and Birkemeier, W., 1996. Bar/trough generation on a natural beach. *J. Geophys. Res.*, 101 (C5), 12097–12110.